

Contents lists available at [ScienceDirect](#)

Food and Bioproducts Processing

journal homepage: www.elsevier.com/locate/fbp

IChemE

Comparative study of red grape must nanofiltration: Laboratory and pilot plant scales

Camila M. Salgado^a, Laura Palacio^a, Pedro Prádanos^{a,*},
Antonio Hernández^a, Carlos González-Huerta^b, Silvia Pérez-Magariño^b

^a Grupo de superficies y Materiales porosos (SMAP, UA-UVA-CSIC), Dpto. de Física Aplicada, Facultad de Ciencias, Universidad de Valladolid, 47011 Valladolid, Spain

^b Instituto Tecnológico Agrario de Castilla y León, Ctra. Burgos Km 119, Finca Zamadueñas, 47071 Valladolid, Spain

A B S T R A C T

A consequence of global warming is the early ripening of grapes which promotes, among others, a higher fermentable sugar (glucose and fructose) content. This leads to wines with an alcoholic degree higher than desired.

In this work, the main differences between red grape must nanofiltration at laboratory and pilot plant scale were studied in order to perform the scale-up of a nanofiltration process to reduce the sugar content. For this, previous results of the nanofiltration of commercial red must using the SR3 membrane in a flat sheet crossflow module were compared with those obtained for the filtration of natural red must using the same membrane in a spiral wound module at two different applied pressures.

The aim of this publication is to analyze the main differences between red grape must nanofiltration at laboratory and at pilot plant scale.

Results: showed that the flow destabilization and eddy promotion caused by spacers in the spiral wound module mitigate the rate at which the cake thickens and compacts on the membrane surface. This causes a less sharp flux decrease, less variable sugars rejection and osmotic pressure difference. Moreover, higher applied pressure promotes a higher membrane fouling and osmotic pressure that worsen the flux decay.

© 2014 The Institution of Chemical Engineers. Published by Elsevier B.V. All rights reserved.

Keywords: Red grape must; Nanofiltration; Scale-up; Spiral wound module; Sugar content reduction

1. Introduction

Membrane processes are now widely considered as economical alternatives to conventional separation processes. Reverse osmosis (RO), nanofiltration (NF), ultrafiltration (UF) and microfiltration (MF) have become standard unit operations (Schwinge et al., 2004).

Membranes can be presented in several configurations such as: spiral wound, hollow fibers, tubular and plate-and-frame modules. Amongst these, the hollow fiber and the spiral wound modules are the most commonly used, due to their high membrane area to volume ratio. Moreover, spiral wound modules are often preferred in industry because they offer a good balance between ease of operation, fouling control,

permeation rate and packing density (Geraldès et al., 2002; Schwinge et al., 2004).

Some membrane processes have been used in winemaking for a long time. For example: cross-flow MF and UF to clarify white grape must (Cassano et al., 2008), sugar concentration using NF (Versari et al., 2003) and RO (Rektor, 2007) in musts. Reverse osmosis is also used to reduce alcohol in wines, unfortunately, RO membranes are permeable to both alcohol and water, and after the filtration it is necessary to add water to the dealcoholized wine which creates legal problems in some countries where the addition of water is forbidden by law (García-Martín et al., 2010).

Furthermore, more recent research and development activities have focused on the application of membrane

* Corresponding author. Tel.: +34 983423739; fax: +34 983423013.
E-mail address: pradanos@termo.uva.es (P. Prádanos).

<http://dx.doi.org/10.1016/j.fbp.2014.08.007>

0960-3085/© 2014 The Institution of Chemical Engineers. Published by Elsevier B.V. All rights reserved.

Nomenclature

Roman

A_{eff}	effective area (m^2)
A_m	membrane active area (m^2)
a_{sp}	specific surface area of the spacer
A_{sp}	surface area of the spacer (m^2)
$C_{0,i}$	feed concentration of the i th component (kg/m^3)
$C_{m,i}$	concentration of the i th component on the membrane active layer (kg/m^3)
$C_{p,i}$	permeate concentration of the i th component (kg/m^3)
C_{RT}	total sugar concentration (glucose and fructose) of the retentate (kg/m^3)
d	dilament thickness (m)
d_h	hydraulic diameter of the channel (m)
D_i	diffusion coefficient of the i th component (m^2/s)
H	feed channel height (m)
J_v	permeate flux per unit of area through the membrane ($m^3/m^2 s$)
J_{v0}	permeate flux per unit of area through the membrane at time $t=0$ ($m^3/m^2 s$)
k	general kinetic constant for the fouling models (s^{-1})
k_c	kinetic constant for the cake model (s/m^6)
$K_{m,i}$	mass transfer coefficient (m/s) of the i th component at impermeable membranes (m/s)
$K_{m,i}^s$	mass transfer coefficient of the i th component at semipermeable membranes (m/s)
L	leaf length (m)
l_m	mesh size (m)
L_p	water permeability (m/Pa s)
M_i	molar weight of the i th component (kg/mol)
n	dimensionless exponent which depends of the fouling model
Q	volumetric recirculation flow (m^3/s)
R	ideal gas constant (1.987×10^{-3} kcal/mol K)
Re	Reynolds number
R_f	resistance due to fouling (m^{-1})
R_i	membranes true retention for the i th component
R_m	membrane resistance (m^{-1})
R_{sys}	system resistance (m^{-1})
Sc	Schmidt number
Sh	Sherwood number
T	absolute temperature (K)
V_0	initial volume of grape must (m^3)
V_p	permeate volume (m^3)
V_{sp}	volume occupied by the spacer (m^3)
V_t	volume of the total (empty) channel (m^3)
W	leaf width (m)

Greek

β	angle between crossing filaments
Δp	applied transmembrane pressure (Pa)
Δp_c	pressure drop across the cake (Pa)
Δp_m	pressure drop across the membrane (Pa)
$\Delta \pi$	osmotic pressure gradient (Pa)
ε	feed spacer porosity
η	viscosity of the solution that passes through the membrane (Pa s)

η_f	feed viscosity (Pa s)
η_p	viscosity inside the membrane pore (Pa s)
θ	angle of the feed flow
v_{eff}	effective velocity (m/s)
ρ_f	feed density (kg/m)

technologies for sugar control in grape musts in order to reduce the alcohol content of the resulting wines (García-Martín et al., 2009, 2010, 2011). As a consequence of global warming, an early ripening of grapes has been detected in some regions that causes higher fermentable sugar (glucose and fructose) content, lower acidities and some modifications of the varietal aroma compounds. Fermentation of this must leads to alcoholic degrees higher than desired (Mira de Orduña, 2010), as they may be too burning in the mouth and mask the fruity aromas and taste of wine. Premature grape harvest and winemaking should affect the final wine quality, leading to more acid and less colored wines, because the phenolic maturity would not be fully achieved (García-Martín et al., 2011). Therefore, in order to produce a full flavored wine, the harvest should be carried out in the optimum ripeness of the fruits and then innovative techniques to control sugars in musts should be applied to keep the alcohol degree of the resulting wines within the desired range. Moreover moderated alcohol contents are becoming a trend in the consumers demand.

If the molecular weight of sugars in must is taken into account, nanofiltration seems to be the most appropriate technique to control the concentration of glucose and fructose (García-Martín et al., 2009). In their work, García-Martín et al. (2010, 2011) studied the sugar reduction of fermentable sugars in musts such as glucose and fructose by a 2 stage nanofiltration process to obtain wines with a slight alcohol reduction. Their results showed that the mixture of the final permeate with the retentate or with untreated must in adequate proportions reduced the alcohol content of the resulting wines by 2°. However, a slight loss of color and aroma intensity and a slender unbalancing of some important substances (i.e. potassium, malic and tartaric acid) were detected. Moreover, these experiments of must nanofiltration, showed that there are some problems specially related with the permeate flux decline.

In our previous work (Salgado et al., 2013), a method was proposed to study the influence of the different compounds present in red grape must on flux decline. Results showed that high molecular weight compounds (namely polyphenols, polysaccharides, proteins, etc) have more influence on the permeate flux decay since they are mainly responsible for the fouling phenomenon (cake filtration mechanism). While low molecular weight compounds (mainly glucose and fructose), contribute to the flux decay mostly through an increase of the osmotic pressure during the process. Aiming to select the most appropriate NF membrane for sugar control in grape must, further research was performed applying the same methodology mentioned in previous works (Salgado et al., 2013). In this work (Salgado et al., 2012), the performance for must nanofiltration of 3 flat sheet NF membranes was compared: the NF270 (Dow Filmtec), HL (GE) and SR3 (Koch Membrane System). The results obtained showed that the HL and SR3 membranes were appropriate to reduce the content of sugar of red must. Specifically, the SR3 membrane showed the best passage of sugar and less fouling. Once the membrane is selected at a laboratory

scale it is reasonable to analyze its performance at a higher scale using a spiral wound module.

The major components of a spiral wound module are the membrane, the feed and permeate channels, spacers in the feed and permeate channels, the permeate tube and the membrane housing (Dickson et al., 1992; Schwinge et al., 2004). The feed flow spacers, which usually consist in non-woven nearly cylindrical filaments, serve to separate adjacent leaves of the membrane and to create flow passages, but also to promote flow unsteadiness and therefore, to enhance mass transport. In this way, the undesirable fouling, concentration polarization and osmotic pressure on the membrane surface are mitigated (Koutsou et al., 2007). The trade-off for a higher mass transfer rate is an increased pressure loss along the feed channel (Schwinge et al., 2004).

The geometry of a spiral wound module is described by the number of leaves, N_L , the leaf length, L , and leaf width, W , of each membrane leaf, the feed channel height, H , and permeate channel height, H_p . The channels heights are defined by the feed and permeate spacer heights. The spacers themselves are characterized by the mesh size, l_m (distance between filaments); filament thickness, d ($d = H/2$); the ratio of them (l_m/d); orientation of the filaments, β ; angle of the feed flow, θ ; hydraulic diameter, d_h , and voidage, ε , the volume of the voids divided by the overall volume (Schock and Miquel, 1987; Schwinge et al., 2004). Fig. 1 provides the top view of a spacer where the geometric characteristics can be appreciated.

The hydrodynamics in a spiral wound module is critically influenced by the presence of the spacer material. Since the height of the feed channel of the spiral wound module is very small (0.5–2 mm), the effect of its curvature on the flow can be neglected and hence the flow can be modeled assuming a thin rectangular channel filled with spacers (Schock and Miquel, 1987). The presence of spacer materials in the channel reduces the void volume and hydraulic diameter (d_h) while raises the effective velocity (v_{eff}).

Furthermore, due to the small spacer height, the circulating velocity does not exceed 0.4 m/s and the pressure drop, recommended by manufacturers, should be between 0.4 and 0.7 bar. Therefore, the Reynolds number, defined on the basis of the average velocity and the spacer filament diameter, is less than 200 (Koutsou et al., 2007).

Due to the low feed flow rates, the role of feed spacers in mass transfer enhancement is of utmost importance (Gerald et al., 2002). Several experimental works in plane-channels containing different periodic arrays of small-diameter cylinders (mimicking spacers) showed that the presence of them caused a flow destabilization (Karniadakis et al., 1988; Koutsou et al., 2004; Zovatto and Pedrizzetti, 2001). In fact, it has been concluded (Karniadakis et al., 1988) that this cylinders act as eddy promoters and their presence leads to the destabilization of the flow by essentially the same mechanism as in rectangular channels but at much lower Reynolds numbers (on the order of hundreds rather than thousands). In more recent studies (Koutsou et al., 2007), the flow inside rectangular channels with non-woven diamond-shaped spacers were studied using direct numerical simulation. The results revealed that, for the range of geometrical parameters examined, the transition Reynolds number occurs at relatively low values: $Re = 35$ –45.

According to other studies (Schock and Miquel, 1987), spacer-filled channels exhibit significantly higher mass transfer rates compared to empty channels over the same range of Reynolds numbers. Further research on the influence

of the geometry of the spacers on the Sherwood number (Koutsou et al., 2009) using numerical simulations and experimental data were performed developing dimensionless correlations for mass transfer coefficients of the usual form, $Sh = a \times Re^m \times Sc^n$ for spacer each geometry.

As mentioned, previous studies at laboratory scale have been performed for the application of nanofiltration in order to control the sugar content of red grape must to produce low alcohol wine (Salgado et al., 2012, 2013). In the present work the scale-up of the selected nanofiltration process is performed as a continuation of the mentioned studies.

The aim of the present publication is to analyze the main differences between red grape must nanofiltration at laboratory and at pilot plant scale using the same membrane. Specifically the fouling mechanisms, sugars rejection and osmotic pressure are compared. The analysis of these processes can be considered as the first stage of the optimization of the procedure for sugar reduction of must at a higher scale.

For this purpose, the previous results obtained for the nanofiltration of commercial red must using the SR3 membrane in a flat sheet crossflow module (Salgado et al., 2012) are compared with those obtained for the filtration of natural red must using the same membrane in a spiral wound module.

Moreover, because in our previous studies (Salgado et al., 2012, 2013) the increase of the osmotic pressure was considered to be a limiting factor of the permeate flux, the study of the increase of the applied transmembrane pressure is relevant. Therefore the effect of the variation of the applied pressure in the performance of the spiral wound module will be also analyzed in order to continue with the optimization process.

2. Theory

2.1. The spiral wound module

2.1.1. Flow conditions in a spiral wound module

As already mentioned, the flow in a spiral wound module can be modeled assuming a thin plane channel filled with spacers, neglecting the effects of the curvature of the module.

The overall voidage fraction (ε) can be evaluated by (Schock and Miquel, 1987; Van Gauwbergen and Baeyens, 1997)

$$\varepsilon = 1 - \frac{V_{sp}}{V_t} \quad (1)$$

where V_{sp} and V_t are the volume occupied by the spacer and the total channel volume, respectively.

V_{sp} and V_t can be calculated by

$$V_{sp} = 0.5 \times \pi \times d^2 \times l_m \quad (2)$$

$$V_t = l_m^2 \times H \quad (3)$$

The effective area, A_{eff} , can be calculated from the leaf width (W), height (H) and porosity (ε) of the spacer as

$$A_{eff} = W \times H \times \varepsilon \quad (4)$$

Therefore, the effective velocity in a spiral wound element can be calculated according to

$$v_{eff} = \frac{Q}{W \times H \times \varepsilon} \quad (5)$$

where Q is the volumetric recirculation flow.

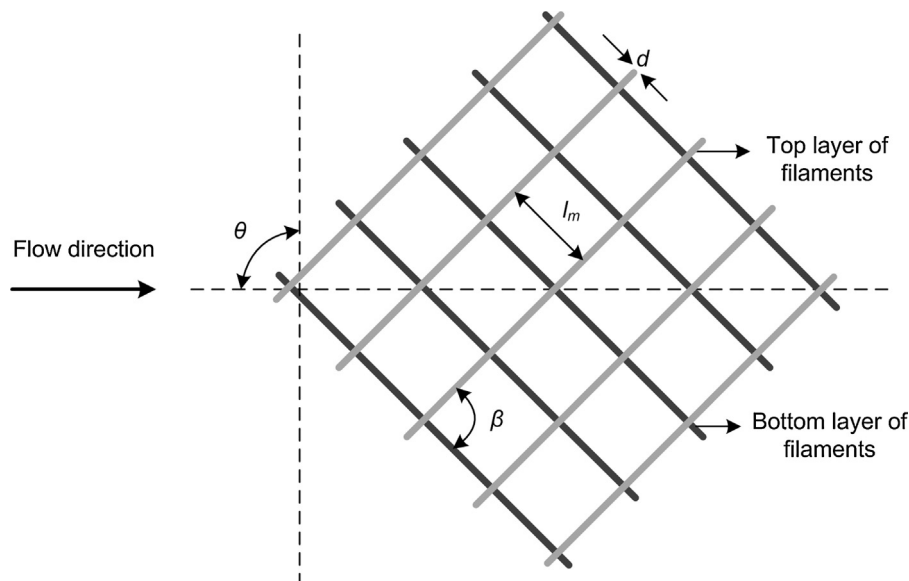


Fig. 1 – Geometric characteristics of a spacer; top view.

For a spacer-filled flat channel the resulting expression for the hydraulic diameter, d_h , is (Schock and Miquel, 1987)

$$d_h = \frac{4 \times \varepsilon}{2/H + (1 - \varepsilon) \times a_{sp}} \quad (6)$$

The specific surface area of the spacer (a_{sp}) is defined as the ratio between its surface area and its volume:

$$a_{sp} = \frac{A_{sp}}{V_{sp}} \quad (7)$$

and A_{sp} is defined as

$$A_{sp} = 2 \times \pi \times l_m \times d \quad (8)$$

2.1.2. Mass-transport in spacer-filled channels

Estimates of the mass transfer coefficient in the presence of different spacers can be obtained (Koutsou et al., 2009) by using the appropriate correlation; that, for the spacer used in the present work, states that the Sherwood (Sh) number can be written in terms of the Reynolds (Re) and Schmidt (Sc) numbers as

$$Sh = 0.14 \times Re^{0.64} \times Sc^{0.42} \quad (9)$$

The Sherwood, Schmidt and Reynolds numbers are defined as

$$Sh = \frac{K_{m,i} d_h}{D_i}, \quad Sc = \frac{\eta_f}{\rho_f D_i}, \quad Re = \frac{v \rho_f d_h}{\eta_f} \quad (10)$$

where, $K_{m,i}$, and D_i are the mass transfer and the diffusion coefficient of the i th component, respectively, and η_f and ρ_f stand for the viscosity and density of the feed, respectively.

Taking into account that the membrane is semipermeable, the value of $K_{m,i}$ calculated using Eqs. (9) and (10), that should be valid for an impenetrable wall, needs to be corrected to $K_{m,i}^s$ according to (Geraldes and Afonso, 2007):

$$K_{m,i}^s = k_{m,i} \left[\left(\frac{Jv}{K_{m,i}} \right) + \left(\frac{Jv/K_{m,i}}{\exp \{Jv/K_{m,i} - 1\}} \right) \right] \quad (11)$$

for $Jv/K_{m,i} \leq 1$

2.2. Permeate flux decrease

When the overall filtration process is taken into account, the flux through the membrane per unit of membrane area can be written in terms of the applied transmembrane pressure, Δp , the osmotic pressure gradient, $\Delta \pi$, the feed viscosity, η_f , and the system resistance, R_{sys} by (Goldsmith, 1971; Jonsson, 1984; Kozinski and Lightfoot, 1971; Wijmans et al., 1984)

$$Jv = \frac{\Delta p - \Delta \pi}{\eta R_{sys}} \quad (12)$$

In filtration processes where the concentration of small and medium sized molecules increases, the flux decreases with time (or filtered volume). This decrease has been attributed to three fundamental factors: the increase of both osmotic pressure and viscosity of the solution that passes through the pores of the membrane and the evolution of the total resistance of the membrane system, $\Delta \pi$, η , and R_{sys} , respectively (Kuhn et al., 2010; Prádanos et al., 1993; Prádanos et al., 1995).

The overall system resistance, R_{sys} , is the sum of the membrane resistance, R_m , plus a series of terms that depend on the fouling caused by the solute and the membrane itself, R_f :

$$R_{sys} = R_m + R_f \quad (13)$$

Assuming that the osmotic pressure follows the van't Hoff's law, the osmotic pressure difference generated by all components can be calculated as

$$\Delta \pi = \sum_{i=1}^N \Delta \pi_i = \sum_{i=1}^N \frac{RT}{M_i} (C_{m,i} - C_{p,i}) \quad (14)$$

where M_i is the molar weight, $C_{m,i}$ the concentration on the membrane surface, $C_{p,i}$ the permeate concentration of the i th component, R the gas constant, and T the temperature. In order to use Eq. (15), it is necessary to calculate the experimentally inaccessible concentration $C_{m,i}$. One of the methods to do this consists in the use of the Film Theory of concentration polarization.

2.3. Concentration polarization. Film theory

This model is based on the use of the mass transfer coefficient, $K_{m,i}$, in order to describe the solute transport in the membrane active layer (Kuhn et al., 2010; Pradanos et al., 1994) as

$$C_{m,i} = C_{p,i} + (C_{0,i} - C_{p,i}) e^{(Jv/K_{m,i})} \quad (15)$$

where Jv is the flux through the membrane defined by Eq. (12); $C_{0,i}$ and $K_{m,i}$ are the feed concentration and the mass transfer coefficient of the i th component, respectively. The last one can be evaluated by Eqs. (9)–(11).

2.4. Fouling mechanism. Cake filtration

The additional resistance attributed to fouling, R_f , has been related with phenomena such as concentration polarization, gelation, deposition, adsorption of solute molecules inside the pores or pore blocking when the pore size is similar to the molecular dimensions (Bowen et al., 1995; Chudacek and Fane, 1984; Hanemaaijer et al., 1988; Seman et al., 2010; Zeman, 1983). All these processes should influence in a more or less balanced equilibrium. They can be accounted by means of four theoretical kinetic models commonly used for systems showing flux decline (Bowen et al., 1995; Pradanos et al., 1996): complete blocking, intermediate blocking, standard filtration and cake filtration models.

In several previous experiments using different flat sheet membranes for grape must nanofiltration (Salgado et al., 2012, 2013), only the very first instants of filtration seemed to be described by an intermediate blocking mechanism.

During, the second and longest step of must nanofiltration, flux decay follows the cake filtration mechanism (Salgado et al., 2013). According to this model, each particle locates on others already arrived and already blocking some pores and there is no room for a direct obstruction of any membrane area. In this case the fouling kinetic constant is k_c (in s/m^6) and can be written as

$$\frac{t}{V_P} = \frac{k_c}{2} V_P + \frac{1}{Jv_0 \cdot A_m} \quad (17)$$

The kinetic constant k_c is twice the membrane fouling index (MFI) (Schippers and Verdouw, 1980) that is defined as the slope of the plot of t/V_P versus V_P .

According to several studies (Listiarini et al., 2009a,b; Sioutopoulos et al., 2010a,b) on fouling of nanofiltration membranes, the cake layer formed on the membrane surface may be compressible and become more compact and dense after a certain period of filtration time or due to an increase of the applied pressure. In fact, another work described that a third mechanism may occur during the flux decline, the so called “cake filtration with compression model” (Schippers and Verdouw, 1980).

2.5. Retention model

The efficiency of a membrane is determined by its true retention, R . This coefficient is defined as

$$R_i = 1 - \frac{C_{p,i}}{C_{m,i}} \quad (i = 1, 2, \dots, N) \quad (18)$$

for the i th component present as solute in the feed. $C_{m,i}$ is the concentration of the i th component on the membrane surface

(membrane active layer) and $C_{p,i}$ the permeate concentration of the i th component.

3. Materials and methods

3.1. Membrane and experimental set-up

The experimental set-up used for must filtrations was similar to the one described in a previous work (Salgado et al., 2013) for the laboratory scale experiments using a flat sheet cross flow module. The main difference, with the scheme presented there, is that the present experiments were performed in a pilot plant scale unit with a spiral wound module of nanofiltration. Briefly, it consists in a feed vessel, with a cryogenic unit to assure that the feed's temperature is kept at 16 °C. The feed is extracted from the thermostated reservoir by means of a regulatable piston membrane pump Hydra—Cell G03. Two pressure transducers are placed before and after the spiral wound module to measure the inlet and outlet pressure. In order to adjust manually the pressure inside the module a needle valve is placed at the exit of the unit. Cross flow is adjusted through this valve and the speed control of the pump. The retentate flow rate is measured with a flowmeter ranging from 0 to 10 L/min. In order to decrease the retentate temperature a heat exchanger was placed before its return to the feed vessel. The permeate flux was monitored using a three-tube flow system with flow capacity from 0 to 10 L/min.

The membrane used for the nanofiltrations was a KMS SR3 (reference 3839 SR3-NYV), made and commercialized by Koch Membrane Systems. The main characteristics of the membrane and the spiral wound module are shown in Tables 1 and 2, respectively. The spacer porosity was assumed to be that determined by Vrouwenvelder et al. (2010) in their work using a diamond-shaped spacer with the same height as the SR3 ($H = 0.787 \times 10^{-3}$ m).

As mentioned, prior to the selection of the SR3 membrane, different nanofiltration membranes in flat sheet configuration were tested using a commercial red must and a synthetic solution containing the main low molecular weight compounds typically found in red must. Results showed that, among the membranes studied, the SR3 presented an appropriate passage of sugars and less fouling (Salgado et al., 2012).

3.2. Must

Tempranillo red grapes from D.O. Rueda were transported to the experimental winery of the Enological Station of Castilla y Leon (Rueda) in plastic boxes of 15 kg. After the reception, grapes were de-stemmed and crushed and sulfite was added (60 mg/L of SO_2). The must was obtained by drawing off, without press. Pectinolytic enzymes (10 mg/L of Novoclear Speed, Lamothe Abiet, France) were added to enhance first clarification. After that, must was filtered through 0.8 μ m cellulose plate filters in order to prevent sudden membrane fouling and to make nanofiltration easier. In this way natural must clarity is similar to that of the commercial must used in the previous experiments with the flat sheet cross flow module.

The main oenological parameters of the red must before the filtration process are shown in Table 3.

3.3. Procedure

Prior to the initial use of the brand new spiral wound module, a cleaning procedure was performed according to the

Table 1 – Nominal data of the SR3 membrane.

MWCO (Da) ^a	Lactose rejection (%) ^a	pH range	Max. pressure (10 ⁵ Pa)	Max. temperature (°C)
200	99,900	3–10	41,400	50,000

^a 5% Lactose at 1380 kPa.**Table 2 – Main characteristics of the SR3 membrane and 3839 SR3-NYV spiral wound module.**

Active membrane area A_m (m ²) ^a	Module length L (m) ^a	Module diameter (m) ^a	Leaf with W (m) ^b	Feed spacer height H (10 ^{−3} m) ^a	Feed spacer porosity ^c (ϵ)
7.061	0.984	0.096	3.608	0.787	0.850

^a Provided by the manufacturer.^b Own determination.^c Vrouwenvelder et al. (2010).**Table 3 – Oenological parameters of the natural red musts before and after the nanofiltration process.**

Must	Glucose (g/L)	Fructose (g/L)	Tartaric acid (g/L)	Malic acid (g/L)	Potassium (mg/L)	pH	Total acidity (g/L)	Total SO ₂ (g/L)
Original must	94.49	97.51	4.82	2.64	930	3.21	5.70	60
Permeate 3100 kPa	25.56	25.91	2.92	2.37	660	3.10	4.18	21
Retentate 3100 kPa	134.74	139.70	4.33	2.55	1050	3.41	4.72	65
Permeate 3300 kPa	23.35	23.76	3.58	2.57	790	3.16	5.01	24
Retentate 3300 kPa	130.14	134.16	4.18	2.36	900	3.28	5.27	68

manufacturer's recommendations in order to remove the preservative solution. Afterwards, to avoid any irreversible change during operation, the membrane was conditioned by pressurization at the highest pressure to be used for a sufficient period of time. In this case, the SR3 was pressurized filtering water at a pressure of 3300 kPa with a recirculation flow of 9 L/min during one hour. After this, water permeability was measured. This parameter was determined before and after every filtration and cleaning cycle.

Filtrations were performed in a batch system. The permeate was sent to the thermostated permeate vessel in order to collect it and the retentate was recirculated to the thermostated feed vessel.

In order to analyze the influence of the applied transmembrane pressure two filtrations were performed the first at 3100 kPa and the second one at 3300 kPa. These two single and close values do not constitute a study of filtration versus pressure but rather have been chosen to show how increasing pressure without providing extra cake disruption media would have detrimental side effects: increasing fouling, worsening flux decay, and increasing osmotic pressure as will be shown below. The rest of the operating conditions for both filtrations were: a feed temperature of 16 °C and a recirculation flow of 9 L/min, which according to Eq. (5) and the spacers dimensions (Table 2) corresponds to an effective velocity of 6.27×10^{-2} m/s. Between filtrations, only one cleaning step was performed, which consisted in a flush cycle with soft water at a recirculation flow of 9 L/min and low pressure using a minimum of three times the system hold-up volume and sending retentate and permeate to the drain.

The permeate flux was determined by measuring the flow, firstly every 15 min and then, when the permeate flux became less variable, every 45 min. Simultaneously, samples of permeate and retentate were taken in order to determine their content of glucose and fructose by liquid chromatography (HPLC).

The volumes filtered where of the order of 35 L of natural red must. Filtrations were performed until the flux decreased to a more or less constant value during a reasonable period of time.

Results of both filtrations were compared with those obtained previously using the same membrane in a flat sheet cross flow module (Salgado et al., 2012).

3.4. Analytical methods

Musts were analyzed before and after filtrations according to the methods summarized in Table 4. With the exception of sugars, malic and tartaric acid, the oenological parameters analyzed were determined according to the Organisation Internationale de la Vigne et du Vin (OIV) methods (OIV, 2011).

According also with the recommendations of OIV (OIV, 2011), potassium was measured by atomic absorption spectrophotometry using an atomic absorption spectrophotometer from Corning, model FP 410, equipped with an air-acetylene burner.

The chromatographic system used consisted in; an HPLC apparatus, with a Refractive Index detector, Waters 2414; an isocratic pump Waters 1515; the Waters 1707 Autosampler; a thermostated column compartment and a control unit commanded by the Breeze 2 software. In order to improve the

Table 4 – Summary of the methods used for the determination of some oenological parameters of musts.

Parameter	Method
Glucose and fructose	HPLC
Tartaric and malic acid	HPLC
pH	pH-meter
Total acidity	Acid–base titration
Total SO ₂	Iodometry
Potassium	Atomic absorption spectroscopy

Table 5 – Hydraulic permeability and membrane resistance, both initially and after filtration and cleaning procedure.

Process	Water Permeability (L_p) (10^{-11} m/Pa s)	Membrane Resistance (R_m) (10^{13} m $^{-1}$)
Before filtration	1.35	7.37
After red must rinse (soft water flush cycle)	0.79	12.65
After manufacturers cleaning procedure	0.89	11.16

resolution and precision, the samples were diluted 1:10 (V/V) with deionized water and then 20 μ L of each were injected in the HPLC system. A Supelco Supelcogel Pb column, and guard column, were used for the sugars (glucose and fructose) separation and a Shodex DE-413 column, and guard column, for malic and tartaric acids detection.

4. Results and discussion

4.1. Permeate flux evolution

As mentioned, water permeability (L_p) was determined before and after the filtrations and cleaning procedure. This parameter was calculated as the slope of the plot of J_v versus Δp by measuring the permeability of the membrane to Milli-Q water at different transmembrane pressures and at 20 °C. The initial and final membrane resistances, R_m , were calculated from L_p data according to Eqs. (12) and (13) when $R_f=0$ and $\Delta T=0$. Results are presented in Table 5. It is shown that after the first red must filtration and rinsing, the water permeability was reduced since the recovery was only 58.3% from the original value. After the cleaning procedure, there is a slight permeability recovery without reaching its original value (66% of the permeability of the brand new membrane). This permanent loss of permeability is attributed to the inevitable and irreversible fouling of the membrane system due to the adsorption of substances on the membrane surface or inside the pores.

The evolution of permeate flux with natural red must as a function of time at both transmembrane pressures is presented in Fig. 2a. As also observed in previous studies with a SR3 flat sheet module (Salgado et al., 2012), both filtrations throughout the spiral wound module follow a typical flux decline kinetic: at the beginning there is a remarkable decrease of flow followed by a less-sharp progressive decay which can be assumed to tend to zero. As expected, higher initial fluxes were measured at the beginning of the filtration at 3300 kPa. But this process presented a faster flux decrease and reached lower values than the one at 3100 kPa. This difference can be attributed to the fact that a higher driving force (transmembrane pressure) accelerates the cake formation on the membrane surface and promotes a higher compaction of it. This issue will be discussed in more detail in Section 4.4. Besides, it has to be taken into account that the first filtration was performed with the brand new membrane, which, as already mentioned, presented less initial fouling. Fig. 2b shows the comparison of the normalized flux decay

using the spiral wound module and the flat sheet membrane module. Even though the later was performed at a higher tangential velocity (2.78 m/s) (Salgado et al., 2012), it is clear that the flat sheet cross flow module reached lower permeate fluxes in a shorter period of time. This issue can be attributed to a faster cake formation and compaction not only due to the higher applied pressure (3500 kPa) but to the absence of spacers that, as already mentioned, mitigate fouling mechanisms.

4.2. Efficiency of the spiral wound module

4.2.1. Analysis of the filtrated musts

Recalling that the aim of the present study is the analysis of the performance of the SR3 spiral wound module for sugar control in grape must, it is essential to analyze the main characteristics of the obtained musts. Therefore, the concentrations of the resultant permeate and retentate were analyzed. Results presented in Table 3 clearly show a high reduction of total sugar content of permeates (about 73%) and an increase in retentates. These variations are not so significant for the rest of compounds. Furthermore, if the purpose of filtration is to reduce the alcohol content of the final wine, the permeate has to be mixed with untreated must or with the retentate in adequate proportions before its fermentation. In this way, the reconstructed must will be chemically very similar to the original one but with a lower sugar content and the variation of the other compounds will be insignificant.

4.2.2. Sugars rejection

Sugar concentration measurements for the permeate and retentate allow the determination of the membrane efficiency by calculating the time evolution of the true retention of each sugar, R_i . True retentions of glucose and fructose have been evaluated according to Eq. (18) and using the equations of mass transport and Film Theory (Eqs. (9)–(11) and (15), respectively). For the density, ρ_f , of red must a correlation between density and its sugar content (°Brix) was taken from the literature (Hidalgo-Togores, 2006). In the case of red must, the viscosity, η_f , values used were obtained by a correlation versus concentration (°Brix) (Zuritz et al., 2005).

The corresponding results are shown in Fig. 3a. It can be noted that there is an almost linear slight decrease of retention of both, glucose and fructose. This true retention time evolution differs from the results obtained in previous experiments using the flat sheet module procedure, where a progressive increase of this parameter was observed (Salgado et al., 2012). A comparison of the rejection of sugars for both the modules is depicted in Fig. 3b, note that the permeate volume is normalized by the feed volume, V_0 , of each filtration. Although it was expected that both systems presented similar initial rejections, it can be appreciated that the flat sheet module system has lower initial retentions (0.181 for glucose and 0.185 for fructose) which increase progressively exceeding the values observed at the beginning of the filtration using the spiral wound module system.

Apparently, the spiral wound module retention is stabilized faster due to an almost instantaneous initial fouling mechanism. Moreover, during the study of the individual effects of low and high molecular weight compounds on the nanofiltration of grape must using a flat sheet membrane, the significant increase of the retention of sugars was also observed in the presence of high molecular weight compounds. This feature was mainly attributed to the formation of the cake layer on the

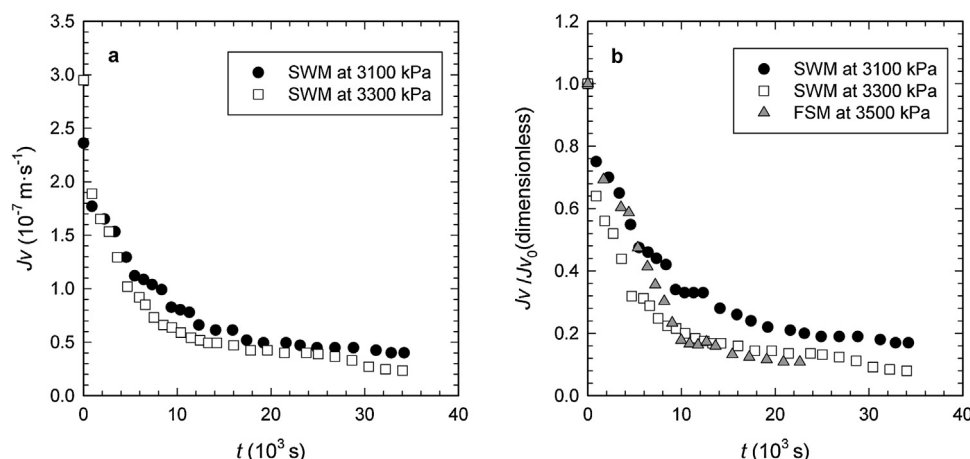


Fig. 2 – Permeate flux time evolution of red must: (a) for the spiral wound module (SWM) at 3100 kPa and at 3300 kPa; (b) normalized for the SWM at 3100 kPa and at 3300 kPa and for the flat sheet module (FSM) at 3500 kPa as a comparison.

membrane surface that acts as a pseudo-membrane which lowers even more the passage of sugars through the membrane by changing both: permeability and selectivity of the overall membrane (Salgado et al., 2013). Taking into account that the effective velocity in the spiral wound module was much lower than in the flat sheet module ($6.27 \times 10^{-2} \text{ ms}^{-1}$ and 2.78 ms^{-1} , respectively), it is possible that the formation of this pseudo-membrane occurs almost instantly due to the lower shear stress that enables a faster deposition of foulants on the membrane surface. Furthermore, in the flat sheet module the progressive increase of R_i would be caused by the thickening of the cake layer on the membrane surface which could not be avoided by the higher shear stress. This corroborates that the presence of feed spacers in the spiral wound module creates local flow structures that periodically disrupt the concentration boundary layers avoiding the thickening of the pseudo-membrane, that is an increase in R_i . Therefore, the slight decrease of the spiral wound module retention could be explained by the increase of sugars concentration on the retentate side that finally crosses the membrane.

All in all, the less variable rejection observed using the spiral wound module is more appropriate for the aim of this study (sugar reduction of red must) because it leads to a low sugar content of the permeate from the beginning of the filtration. Furthermore, J_v is higher and therefore more V_P with the appropriate sugars concentration is collected.

4.3. Resistance to the permeate flux

The resistance to permeate flux due to fouling, R_f , was determined according to Eqs. (12) and (13), assuming that R_m increases linearly with time (Salgado et al., 2013). Fig. 4 shows the results obtained as a function of the filtration time. Here, it can be noticed that there is a slight difference between both the applied pressures. During the filtration at 3100 kPa, R_f increases progressively until reaching a maximum, beyond which there is a slight decrease and possible stabilization. A similar evolution of R_f was observed during the filtration using the SR3 flat sheet module (Salgado et al., 2012). At 3300 kPa, this parameter grows continuously reaching higher values and no decay is observed. As reported in previous studies (Foley et al., 1995; Salgado et al., 2013), a reduction in the resistance due to the cake formation can be caused by an increase of the osmotic pressure. For this purpose it has to be considered that the overall pressure drop (applied trans-membrane pressure Δp) at any time is the sum of pressure drops through the membrane, Δp_m , and cake, Δp_c , plus the osmotic pressure, $\Delta \pi$. Besides when the cake has an appreciable thickness, Δp_m is small in comparison with Δp_c . So, a reduction in the effective pressure across the total membrane system could be due to a reduction of the cake pressure drop, Δp_c (and so in R_f) that may occur due to an increase in osmotic pressure.

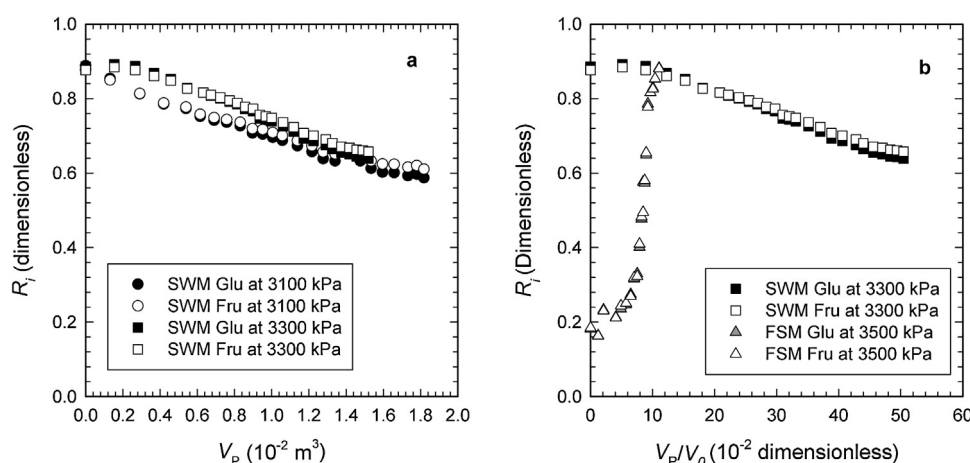


Fig. 3 – True glucose (Glu) and fructose (Fru) retentions: (a) as a function of permeate volume (V_P) for the spiral wound module (SWM) at 3100 kPa and at 3300 kPa; (b) as a function of the normalized volume for the SWM at 3300 kPa and for the flat sheet module (FSM) at 3500 kPa as a comparison.

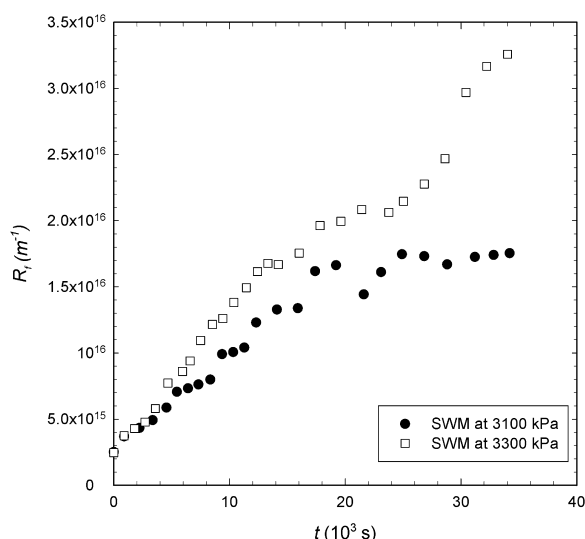


Fig. 4 – Time evolution of the resistance to the permeate flux due to fouling (R_f) for the spiral wound module (SWM) at 3100 kPa and at 3300 kPa.

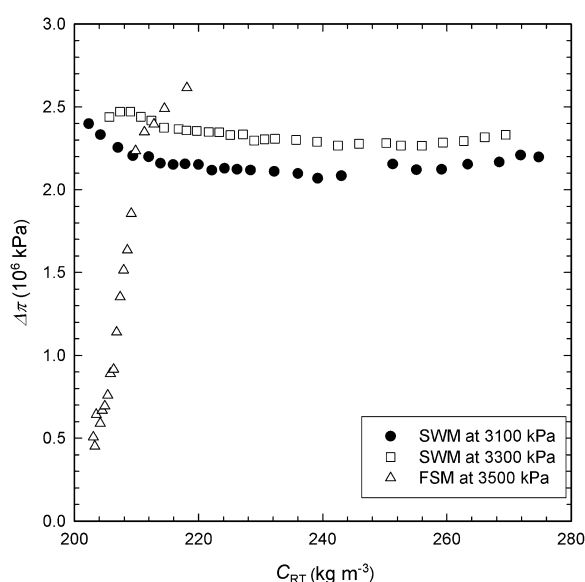


Fig. 5 – Osmotic pressure difference as a function of the total sugars content of the retentate (C_{RT}) for the spiral wound module (SWM) at 3100 kPa and at 3300 kPa and for the flat sheet module (FSM).

Therefore, it was logic to expect a decrease in resistance for lower transmembrane pressures. Moreover, a higher applied pressure may cause the formation of a more compact cake layer on the membrane surface contributing also to higher values of R_f .

In order to analyze the influence of the osmotic pressure, the values calculated according to Eq. (14) were plotted as a function of the total sugars content of the retentate (C_{RT}) in Fig. 5. In this case, no significant osmotic pressure variation can be appreciated. On the contrary, in studies using flat sheet modules, it was observed that this parameter increased remarkably during filtration (Salgado et al., 2012, 2013) reaching higher values than in the spiral wound module. The values obtained for the SR3 flat sheet module are presented in Fig. 5 for the sake of comparison. This shows that, as mentioned in Section 4.2.2, spacers increase shear rates, and mass transfer. Therefore, phenomena such as fouling, concentration polarization and osmotic pressure on the membrane surface are

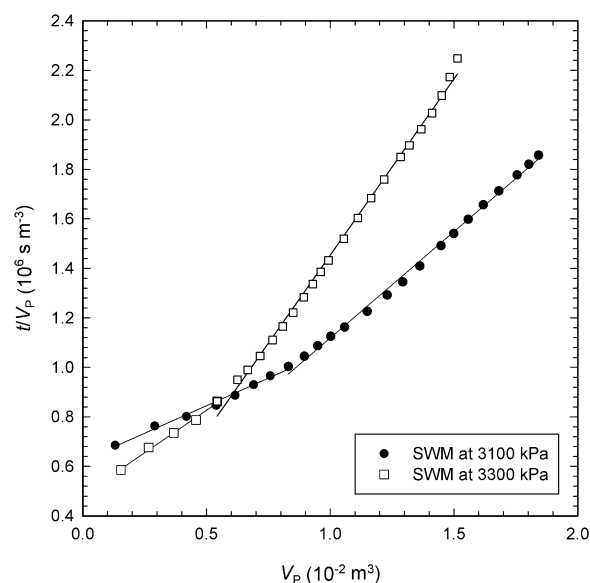


Fig. 6 – (t/V_p) versus V_p fitted to the cake filtration model for the spiral wound module (SWM) at 3100 kPa and at 3300 kPa. The kinetic constants: k_{c1} and k_{c2} , for both filtrations, correspond to the slope of the region of cake formation and cake formation with compaction, respectively.

mitigated in the long term, and so the thickening of the cake layer is limited. This promotes more stable sugar retention and osmotic pressure difference. By contrast, in the flat sheet membrane filtration, the absence of local flow structures causes the progressive thickening of the cake layer, and consequently less constant osmotic pressure and sugar rejection.

4.4. Fouling mechanism

A description of the flux decline presented in Fig. 2 can be performed in terms of the outlined fouling mechanisms. The fitting of the experimental data to the cake filtration mechanism (Eq. (17)) is plotted in Fig. 6. It is observed that for both filtrations the cake filtration model satisfactorily describes the experimental data for almost the entire filtration period and seems to be divided in two regions, the so called: cake formation and cake formation with compaction (Schippers and Verdouw, 1980). Similar results were obtained during the filtration of red must using the flat sheet module (Salgado et al., 2012). As mentioned elsewhere (Salgado et al., 2013), during the first minutes of must filtration (or the first $1.5 \times 10^{-3} \text{ m}^3$ of permeated volume) other fouling mechanism as the intermediate blocking could be expected to play a dominant role, but in the present case the process is so fast that any other mechanism rather than cake couldn't be appreciated.

In order to compare the cake formation kinetic constants (k_{c1} and k_{c2}) of both filtrations along the complete experiments, the slope of each region in the plot (t/V_p) versus V_p (Fig. 6) was obtained. Results are presented in Table 6, where it is apparent that the filtration performed at 3300 kPa presented a higher slope, that is higher cake formation kinetic constants in both regions (k_{c1} and k_{c2}). This agrees with the flux decline analyzed in Section 4.1 where even though filtration at 3300 kPa presented a higher initial flux it also reached lower values. Therefore it may be said that the initial flux has a clear effect on the rate of fouling since it affects the rate at which fouling species are brought to the membrane surface.

Table 6 – Cake formation kinetic constants of both cake filtration mechanism regions for the spiral wound module and flat sheet module. Values were obtained as the slope of the plot t/V_p versus V_p for each region in the three filtration processes.

Module	Applied pressure Δp (kPa)	k_{c1} (s/m ⁶)	k_{c2} (s/m ⁶)
Spiral wound	3100	8.902×10^7	1.718×10^8
Spiral wound	3300	1.374×10^8	2.847×10^8
Flat sheet ^a	3500	1.475×10^{11}	8.422×10^{11}

^a Salgado et al. (2012).

Furthermore, high initial fluxes increase cake compaction and consequently the resistance to the permeate flux (R_f) as mentioned in Section 4.3. This agrees with the results presented in other studies of the influence of initial flux on membrane fouling (Sioutopoulos et al., 2010b). There they concluded that the greater the initial rate, the more severe the fouling of the membrane.

Aiming to analyze the differences of the fouling mechanism between both modules, the results of the cake formation kinetic constants (k_{c1} and k_{c2}) obtained in previous experiments (Salgado et al., 2012) for the flat sheet module are presented in Table 6. It is clear that k_{c1} and k_{c2} are around 1000 times higher for the flat sheet module. This agrees with the fact that a higher driving force (applied pressure) promotes the rate of fouling and cake compaction. This also corroborates the analysis made in the previous Sections 4.2.2 and 4.3. Even though the formation of the pseudo-membrane is faster in the spiral wound module, the flow destabilization and eddy promotion caused by the spacers mitigates the rate at which the cake thickens on the membrane surface.

5. Conclusions

The comparison of the performance of both modules allowed the analysis of the influence of feed spacers on fouling mechanism, time evolution of sugar retention and osmotic pressure during must nanofiltration.

Even though the formation of the pseudo-membrane is faster in the spiral wound module, probably due to a lower tangential velocity, the flow destabilization and eddy promotion caused by the spacers mitigates the rate at which the cake thickens and compacts on the membrane surface. The latter causes a less-sharp J_v decrease with more appropriate almost constant sugars rejection and small osmotic pressure differences.

Since the latter features were obtained at a lower recirculation flow than with the flat sheet module, it can be concluded that the spiral wound module is more energy efficient too.

The results obtained for the filtrations performed with the spiral wound module show that a higher applied pressure promotes cake formation and compaction and therefore a higher fouling resistance and osmotic pressure that worsen the decrease of J_v . Therefore, the optimization of the system wouldn't consist in a simple increase of the applied transmembrane pressure but in promoting higher shear stress (presumably with a higher effective velocity) on the membrane surface combined with higher driving force (applied pressure). Thus, J_v would be increased and polarization would be

mitigated decreasing also the resistance toward mass transport (i.e. osmotic pressure and fouling).

Acknowledgments

Authors would like to thank the Ministerio de Ciencia e Innovación (MCINN) for the financial support of this work within the frame of the “Plan Nacional de I+D+I” through the research projects CTQ2009-07666, CTQ2012-31076 and MAT2010-20668. We also are grateful to the projects: VA-324A11-2 of the Junta de Castilla y León, and RTA2012-00092-C02 from the INIA of the MICINN. The company Acciona Agua partially founded this research too.

C. Salgado wants to thank the Spanish Ministry of Education for the grant they gave to her within the frame of the “Plan Nacional de Investigación Científica, Desarrollo e Innovación Tecnológica 2008–2011” (FPU grant: AP2010-5769) to complete her PhD.

References

- Bowen, W.R., Calvo, J.I., Hernández, A., 1995. Steps of membrane blocking in flux decline during protein microfiltration. *J. Membr. Sci.* 101, 153–165.
- Cassano, A., Mecchia, A., Drioli, E., 2008. Analyses of hydrodynamic resistances and operating parameters in the ultrafiltration of grape must. *J. Food Eng.* 89, 171–177.
- Chudacek, M.W., Fane, A.G., 1984. The dynamics of polarisation in unstirred and stirred ultrafiltration. *J. Membr. Sci.* 21, 145–160.
- Dickson, J.M., Spencer, J., Costa, M.L., 1992. Dilute single and mixed solute systems in a spiral wound reverse osmosis module Part I: Theoretical model development. *Desalination* 89, 63–88.
- Foley, G., Malone, D.M., MacLoughlin, F., 1995. Modelling the effects of particle polydispersity in crossflow filtration. *J. Membr. Sci.* 99, 77–88.
- García-Martín, N., Palacio, L., Prádanos, P., Hernández, A., Ortega-Heras, M., Pérez-Magariño, S., González-Huerta, D.C., 2009. Evaluation of several ultra- and nanofiltration membranes for sugar control in winemaking. *Desalination* 245, 554–558.
- García-Martín, N., Perez-Magarino, S., Ortega-Heras, M., Gonzalez-Huerta, C., Mihnea, M., Gonzalez-Sanjose, M.L., Palacio, L., Prádanos, P., Hernandez, A., 2011. Sugar reduction in white and red musts with nanofiltration membranes. *Desalin. Water Treat.* 27, 167–174.
- García-Martín, N., Perez-Magariño, S., Ortega-Heras, M., González-Huerta, C., Mihnea, M., González-Sanjosé, M.L., Palacio, L., Prádanos, P., Hernández, A., 2010. Sugar reduction in musts with nanofiltration membranes to obtain low alcohol-content wines. *Sep. Purif. Technol.* 76, 158–170.
- Geraldes, V., Afonso, M.D., 2007. Prediction of the concentration polarization in the nanofiltration/reverse osmosis of dilute multi-ionic solutions. *J. Membr. Sci.* 300, 20–27.
- Geraldes, V.t., Semiao, V., de Pinho, M.N., 2002. Flow management in nanofiltration spiral wound modules with ladder-type spacers. *J. Membr. Sci.* 203, 87–102.
- Goldsmith, R.L., 1971. Macromolecular ultrafiltration with microporous membranes. *Ind. Eng. Chem. Fundam.* 10, 113–120.
- Hanemaaijer, J.H., Robbertsen, T., Van Den Boomgaard, T., Olieman, C., Both, P., Schmidt, D.G., 1988. Characterization of clean and fouled ultrafiltration membranes. *Desalination* 68, 93–108.
- Hidalgo-Togores, J., 2006. *Calidad del vino desde el viñedo*. Mundi-Prensa, Madrid.
- Jonsson, G., 1984. Boundary layer phenomena during ultrafiltration of dextran and whey protein solutions. *Desalination* 51, 61–77.

- Karniadakis, G.E., Mikic, B.B., Patera, A.T., 1988. Minimum-dissipation transport enhancement by flow destabilization: Reynolds' analogy revisited. *J. Fluid Mech.* 192, 365–391.
- Koutsou, C.P., Yiantsios, S.G., Karabelas, A.J., 2004. Numerical simulation of the flow in a plane-channel containing a periodic array of cylindrical turbulence promoters. *J. Membr. Sci.* 231, 81–90.
- Koutsou, C.P., Yiantsios, S.G., Karabelas, A.J., 2007. Direct numerical simulation of flow in spacer-filled channels: effect of spacer geometrical characteristics. *J. Membr. Sci.* 291, 53–69.
- Koutsou, C.P., Yiantsios, S.G., Karabelas, A.J., 2009. A numerical and experimental study of mass transfer in spacer-filled channels: effects of spacer geometrical characteristics and Schmidt number. *J. Membr. Sci.* 326, 234–251.
- Kozinski, A.A., Lightfoot, E.N., 1971. Ultrafiltration of proteins in stagnation flow. *AIChE J.* 17, 81–85.
- Kuhn, R.C., Maugeri Filho, F., Silva, V., Palacio, L., Hernández, A., Prádanos, P., 2010. Mass transfer and transport during purification of fructooligosaccharides by nanofiltration. *J. Membr. Sci.* 365, 356–365.
- Listiari, K., Chun, W., Sun, D.D., Leckie, J.O., 2009a. Fouling mechanism and resistance analyses of systems containing sodium alginate, calcium, alum and their combination in dead-end fouling of nanofiltration membranes. *J. Membr. Sci.* 344, 244–251.
- Listiari, K., Sun, D.D., Leckie, J.O., 2009b. Organic fouling of nanofiltration membranes: evaluating the effects of humic acid, calcium, alum coagulant and their combinations on the specific cake resistance. *J. Membr. Sci.* 332, 56–62.
- Mira de Orduña, R., 2010. Climate change associated effects on grape and wine quality and production. *Food Res. Int.* 43, 1844–1855.
- OIV, 2011. *Compendium of International Methods of Wine and Must Analysis*. OIV, Paris.
- Prádanos, P., Arribas, J.I., Hernández, A., 1993. Flux limiting factors in cross-flow ultrafiltration of invertase through an asymmetric inorganic membrane. *Sep. Sci. Technol.* 28, 1899–1911.
- Prádanos, P., Arribas, J.I., Hernández, A., 1994. Retention of proteins in cross-flow UF through asymmetric inorganic membranes. *AIChE J.* 40, 1901–1910.
- Prádanos, P., de Abajo, J., de la Campa, J.G., Hernández, A., 1995. A comparative analysis of flux limit models for ultrafiltration membranes. *J. Membr. Sci.* 108, 129–142.
- Prádanos, P., Hernández, A., Calvo, J.I., Tejerina, F., 1996. Mechanisms of protein fouling in cross-flow UF through an asymmetric inorganic membrane. *J. Membr. Sci.* 114, 115–126.
- Rektor, A., 2007. Pilot plant RO-filtration of grape juice. *Sep. Purif. Technol.* 57, 473.
- Salgado, C., Carmona, F.J., Palacio, L., Prádanos, P., Hernández, A., 2012. Evaluation of nanofiltration membranes for sugar reduction in red grape must. In: *Euromembrane 2012*, London, UK.
- Salgado, C., Palacio, L., Carmona, F.J., Hernández, A., Prádanos, P., 2013. Influence of low and high molecular weight compounds on the permeate flux decline in nanofiltration of red grape must. *Desalination* 315, 124–134.
- Schippers, J.C., Verdouw, J., 1980. The modified fouling index, a method of determining the fouling characteristics of water. *Desalination* 32, 137–148.
- Schock, G., Miquel, A., 1987. Mass transfer and pressure loss in spiral wound modules. *Desalination* 64, 339–352.
- Schwinge, J., Neal, P.R., Wiley, D.E., Fletcher, D.F., Fane, A.G., 2004. Spiral wound modules and spacers: review and analysis. *J. Membr. Sci.* 242, 129–153.
- Seman, M.N.A., Khayet, M., Hilal, N., 2010. Nanofiltration thin-film composite polyester polyethersulfone-based membranes prepared by interfacial polymerization. *J. Membr. Sci.* 348, 109–116.
- Sioutopoulos, D.C., Karabelas, A.J., Yiantsios, S.G., 2010a. Organic fouling of RO membranes: Investigating the correlation of RO and UF fouling resistances for predictive purposes. *Desalination* 261, 272–283.
- Sioutopoulos, D.C., Yiantsios, S.G., Karabelas, A.J., 2010b. Relation between fouling characteristics of RO and UF membranes in experiments with colloidal organic and inorganic species. *J. Membr. Sci.* 350, 62–82.
- Van Gauwbergen, D., Baeyens, J., 1997. Macroscopic fluid flow conditions in spiral-wound membrane elements. *Desalination* 110, 287–299.
- Versari, A., Ferrarini, R., Parpinello, G.P., Galassi, S., 2003. Concentration of grape must by nanofiltration membranes. *Food Bioprod. Process.* 81, 275–278.
- Vrouwenvelder, J.S., Picioreanu, C., Kruithof, J.C., van Loosdrecht, M.C.M., 2010. Biofouling in spiral wound membrane systems: three-dimensional CFD model based evaluation of experimental data. *J. Membr. Sci.* 346, 71–85.
- Wijmans, J.G., Nakao, S., Smolders, C.A., 1984. Flux limitation in ultrafiltration: osmotic pressure model and gel layer model. *J. Membr. Sci.* 20, 115–124.
- Zeman, L.J., 1983. Adsorption effects in rejection of macromolecules by ultrafiltration membranes. *J. Membr. Sci.* 15, 213–230.
- Zovatto, L., Pedrizzetti, G., 2001. Flow about a circular cylinder between parallel walls. *J. Fluid Mech.* 440, 1–25.
- Zuritz, C.A., Puentes, E.M., Mathey, H.H., Pérez, E.H., Gascón, A., Rubio, L.A., Carullo, C.A., Chernikoff, R.E., Cabeza, M.S., 2005. Density, viscosity and coefficient of thermal expansion of clear grape juice at different soluble solid concentrations and temperatures. *J. Food Eng.* 71, 143–149.